JOURNAL OF MARINE SCIENCES & ENVIRONMENTAL TECHNOLOGIES
Vol. 8, Issue No. 1 (June-2022)

ISSN (Print): 2413-5267
ISSN (Online): 2706-9966

Analytical Approach for Estimation of Wave Transmission Coefficient for Π-Shaped Floating Breakwater

Abubaker Alamailes

Department of Civil Engineering, Faculty of Engineering, Misurata University, Misurata, Libya.

E-mail: a.alamailes@eng.misuratau.edu.ly

مقاربة تحليلية لتقدير معامل انتقال الموجة لحاجز أمواج عائم على شكل الحرف اللاتينيII

أبوبكر على الأميلس

قسم الهندسة المدنية، كلية الهندسة، جامعة مصراتة، مصراتة، ليبيا.

Received: 30 May 2022; Revised: 22 June 2022; Accepted: 28 June 2022.

Abstract

This study presents a simplified analytical approach, based on power transmission theory, to estimate the transmission coefficient of a π-shaped floating breakwater (FB) with finite width. In evaluating the transmitted wave power, this approach considers both the incident wave kinetic power and the heave oscillation of the FB. Additional power due to the acceleration of the floating body and the hydrodynamic mass increases the transmitted wave power behind the FB and consequently increases the transmission coefficient. The proposed theoretical approach is validated using laboratory-scale experimental data obtained from the literature for π-shaped FB. The results of the proposed approach are in good to excellent agreement with those of experimental studies. In addition, the reliability of the proposed approach is assessed by comparing its results with those of other theoretical models. The effects of sea depth, relative draft, and incident wave height on the magnitude of the transmission coefficient are examined. It is found that the effect of the incident wave height distinguishes the proposed model from others in the existing literature.

Keywords: *Floating structure, Hydrodynamic mass, Incident power, Transmission coefficient, Wave transmission.*

الملخص

تقدم هذه الدراسة مقاربة تحليلية مبسطة، مبنية على نظرية انتقال طاقة الموجة لتقدير قيمة معامل انتقال الأمواج لحاجز أمواج عائم محدود العرض على شكل الحرف اللاتيني II. عند تقييم طاقة الموجة المنتقلة، تأخذ هذه المقاربة في الاعتبار كل من الطاقة الحركية للموجة المتقدمة، والحركة التذبذبية في الاتجاه الرأسي لحاجز الأمواج العائم. تزيد الطاقة الإضافية الناتجة عن تسارع المنشأ العائم والكتلة الهيدروديناميكية من طاقة الموجة المنتقلة خلف هذا المنشأ، وبالتالي تزيد من قيمة معامل انتقال الموجة. تم التحقق من صحة المقاربة التحليلية المقترحة باستخدام البيانات المعملية التي تم الحصول عليها من عدد من الدراسة المعملية السابقة التي أجريت على هذا النوع من حواجز الأمواج العائمة. بينت نتائج المقاربة التحليلية توافق جيد إلى ممتاز مع نتائج الدراسات العملية، بالإضافة إلى ذلك، تم تقييم موثوقية المقاربة المقترحة في هذه الدراسة من خلال مقارنة نتائجها مع نتائج عدد من المقاربات النظرية الأخرى. تم دراسة تأثير التغير في عمق البحر، والغاطس النسبي للحاجز العائم، وارتفاع الموجة المتقدمة على قيمة معامل انتقال الموجة. ولقد وجد أن تأثير ارتفاع موجة المتقدمة يميز المقاربة التحليلية لهذه الدراسة عن غيره من المقاربات النظرية الأخرى.

الكلمات الدالة: المنشأ العائم، الكتلة الهيدروديناميكية، طاقة الموجة المتقدمة، معامل الانتقال، انتقال الموجة.

ISSN (Print): 2413-5267
ISSN (Online): 2706-9966

1. Introduction

Floating breakwaters (FBs) are offshore structures, among others, developed to reduce the impact of waves by reflecting and dissipating the incident wave power. Numerous studies have experimentally investigated the hydrodynamic performance of floating structures by optimizing wave attenuation behind WECs and estimating the impact of the transmitted waves on the coastline (Venugopal & Smith, 2007; Palha *et al*., 2010; Beels *et al*., 2010; Ruol *et al*., 2011; and Diaconu & Rusu, 2013).

The commonly accepted standard for evaluating the performance of a FB is the transmission coefficient (K_t), which is the ratio of the transmitted wave height (H_t) to the incident wave height (H_i). In linear wave theory, the transmission coefficient can also be defined as the square root of the transmitted wave power (P_t) over the incident wave power (P_i) (Hales, 1980; McCartney, 1985; and Türker & Kabdasli, 2004).

Some simplified approaches have been derived from linear wave theory to estimate the performance of FBs. In general, these approaches provide a fair preliminary estimation of the transmission coefficient. One of the first such studies was performed in 1947 by Ursell, who established a theory for the partial transmission and reflection of waves in deep water for rigid and fixed submerged structures with extremely small widths. Ursell used the modified Bessel function to obtain a simple formula for calculating the structure's transmission coefficient. Another well-known formula was developed by Macagno (1954), who assumed a rigid, fixed, and finite-width structure installed in deep water. Several years later, Wiegel (1960) developed the power transmission theory, which assumes that all of the incident wave power between the structure draft and the seabed is fully transmitted. The transmitted power considered in this theory is only the power associated to the wave-induced pressure. While the wave power is typically attributed to pressure forces (Sorensen, 2005), in reality there are contributions arising from the transport of the kinetic and potential wave energies (Holthuijsen, 2010). Wiegel's theory ignored the effect of the transport of the wave kinetic energy and disregarded the effect of the oscillating motion of the floating body, and based on this approximation, the transmission coefficient is estimated as;

$$K_t = \sqrt{\frac{Transmitted\ \ induced\ pressure\ part\ of\ wave\ power}{incident\ induced\ pressure\ part\ of\ wave\ power}} \quad \ldots\ldots (1)$$

Later *et al.* (1996) modified Wiegel's theory by including partial wave reflection in the definition of the transmission coefficient. The researchers assumed that the wave-induced pressure under the floating structure equals the sum of the incident wave-induced pressure and the reflected wave-induced pressure. Findings using this approach exhibit a higher net pressure under the structure than was assumed by Wiegel. In contrast, the orbital horizontal velocity, which is modified by subtracting the reflective horizontal velocity from the incident horizontal velocity, is slower than the orbital horizontal velocity assumed by Wiegel.

ISSN (Print): 2413-5267
ISSN (Online): 2706-9966

Ruol *et al.* (2013) developed a model for π-shaped FBs and later found that this model was also applicable to box-shaped FBs. This approach introduced a modification factor based on an experimental dataset and a function of the relative wave period into Macagno's formula. The researchers considered the impact of the heaving motion of the FB in estimating the transmission coefficient.

Several experimental investigations and computer-based numerical studies have been conducted to evaluate the wave attenuation capabilities of different floating structures. For example, Li *et al.* (2005) numerically modeled the wave transmission characteristics past infinitely long cylindrical and rectangular floating objectives by modifying Tsay and Liu's approach (Tsay and Liu, 1983). Dong *et al*. (2008) tested a two-dimensional (2D) physical model to measure the wave transmission coefficients of single box, double box, and board net breakwaters under regular waves. He *et al*. (2012) experimentally compared the transmission coefficients of FBs with pneumatic chambers to those of regular box-type FBs. The physical models were tested under regular waves with different heights and periods and at various water depths. More recently, Ji *et al*. (2015) proposed cylindrical FBs (CFBs) and experimentally examined their wave attenuation performance.

In all these theoretical approaches, the effect of the kinetic part of the wave power has been ignored when evaluating the hydrodynamic performance and estimating the transmission coefficient of floating structures. Moreover, most of these theories ignore the floating structure's movement. The present study proposes a simple theoretical approach for estimating the transmission coefficient of relatively wide π-shaped floating structures using the power transmission theory and considering the kinetic part of wave power as a variable that affects the magnitude of the transmission coefficient. In addition, the hydrodynamic (added) mass effect resulting from the heaving motion of the floating structure is considered. The additional kinetic energy flux is expected to increase the effect of the kinetic part of the incident wave power.

In general, floating structures have six degrees of freedom. This study considers only heave oscillation, as it always occurs and is not significantly affected by mooring systems (Ruol *et al*., 2013). The transmission coefficient calculated using the present approach is validated by laboratory-scale experimental data obtained from two studies on π-shaped FBs performed by (Koutandos *et al*., 2005; & Cox *et al*., 2007). In addition, to assess the reliability of the proposed model, the transmission coefficient is compared with those calculated by other researchers, including Macagno (1954), Kriebel & Bollmann (1996), and Ruol *et al*. (2013).

As with other theoretical models, the approach of this study is derived using a 2D assumption and validated using 2D experimental data. Thus, diffraction effects due to the floating structure's finite length are not considered. Nevertheless, in practice, floating structures are usually connected to each other or arranged such that they can be considered as a single long body. The effects of the wave propagating angle and the layouts of floating structures on the transmission coefficient have been investigated by Martinelli *et al*. (2008) and Diamantoulaki & Angelides (2011).

ISSN (Print): 2413-5267
ISSN (Online): 2706-9966

2. Methodology

Wave decay on floating structures can be related to the ratio between incoming wave height (H_i) and transmitted wave height (H_t). As a wave passes a floating structure, it decays and attains new height (H_t). Such wave attenuation can be expressed by the wave transmission coefficient (K_t) as;

$$K_t = \frac{H_t}{H_i} \quad \ldots\ldots (2)$$

The transmission coefficient can range from 0 to 1, where 0 indicates no transmission and 1 indicates complete transmission (*i.e.*, no energy loss). The dimensionless transmission coefficient can be defined as a function of flow, fluid, and structure properties, and can also be defined in terms of incident and transmitted wave energies using power transmission theory (Türker, 2014).

In case of tall and wide floating structures, overtopping is unlikely to occur; in this case, the wave transmission depends on the amount of wave power transmitted to the lee side from underneath the floating structure.

The incident wave energy includes potential, kinetic, and wave-induced pressure energy. Under the assumptions of linear wave theory, the energy transport (wave power) in the wave propagation direction is estimated by considering only the work done by the wave-induced pressure, yielding the well-known equation for wave power per unit wave length:

$$P_{Incident} = \frac{1}{8}\,\rho\, g H^2 \;\; \frac{1}{2}\left[1 + \frac{2kd}{\sinh(2kd)}\right]\frac{\omega}{k} \quad \ldots\ldots (3)$$

where, H is the wave height, d is the water depth, ρ is the fluid density, g is the gravitational acceleration, ω is the wave circular or radian frequency (= $2\pi/T$), k is the wave number (= $2\pi/L$), T is the wave period, and L is the wave length.

Eqn. (3) is obtained by ignoring the transport of kinetic energy (kinetic part of the wave power), owing to approximation to a certain order of accuracy (Holthuijsen, 2010). However, in the presence of floating structures, the kinetic part of the wave power should be considered because their heaving behavior significantly affects the total transmitted power. Therefore, the kinetic part of the wave power together with the kinetic energy flux generated from the heaving oscillation of the floating structures increase the total transmitted power and hence, the transmission coefficient. Therefore, the total incident wave power $P_{I.tot}$ comprises the kinetic part of the wave power $P_{I.1}$ in addition to the wave-induced pressure part $P_{I.2}$.

Some of these two wave powers is transmitted from beneath the floating structure draft D to the lee side (Fig. 1). The transmitted part includes the kinetic energy contribution to the wave power $P_{T.1}$ and the induced pressure energy contribution ($P_{T.2}$). In addition to $P_{T.1}$ and $P_{T.2}$, the kinetic energy flux per unit floating structure width resulting from the heaving motion of the floating structure ($P_{T.3}$) is transmitted in the x direction to the lee side. $P_{T.3}$ consists of two

ISSN (Print): 2413-5267
ISSN (Online): 2706-9966

contributions: the kinetic energy flux of the heaving body of the floating structure and the kinetic energy flux of the hydrodynamic mass that accelerates simultaneously with the floating body.

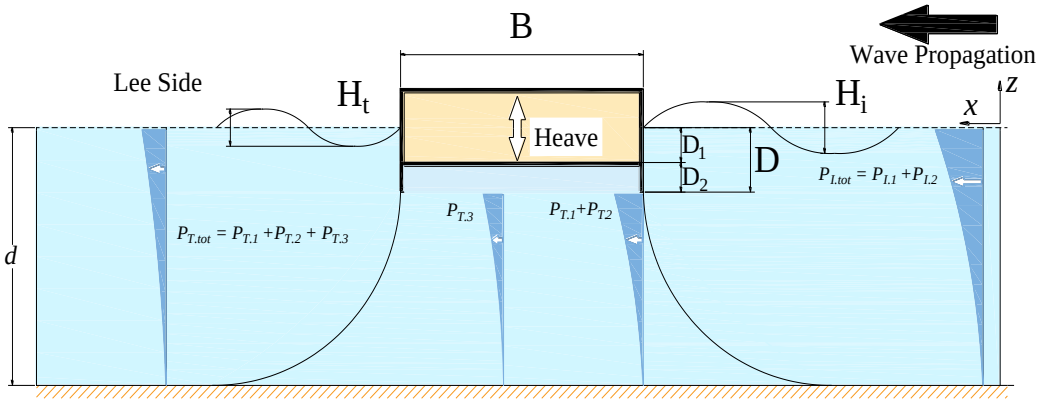

Figure 1. Wave transmission process for π-shaped floating structures.

The transmitted wave (at the lee side of the floating structure) carries a total power that equals the total transmitted power ($P_{T.tot} = P_{T.1} + P_{T.2} + P_{T.3}$). The transmitted wave becomes the incident wave toward the coastline with a height of H_t, which is attained after attenuation of the seaside incident wave. The leeside incident wave carries a total power $P_{L.S}$ that comprises the wave-induced pressure and kinetic parts of wave power. $P_{L.S}$ is a function of H_t, and once the value of $P_{L.S}$ is found (i.e., $P_{L.S} = P_{T.tot}$), the value of H_t can be obtained and the transmission coefficient K_t can be calculated using Eqn. (2).

3. Incident Wave Power

The presence of a wave at the water surface indicates that water particles have been induced to move from their position at rest to some other position. The change in the position of these particles requires that work be done against gravity, which represents potential energy. Moreover, the movement of water particles represents kinetic energy. Therefore, total wave energy (E) is equal to the sum of the potential energy (E_{po}), and kinetic energy (E_k) (Sorensen, 2005):

$$E = E_{po} + E_k = \frac{1}{8}\rho g H^2 \quad \ldots\ldots (4)$$

As the waves propagate across the water's surface, they carry potential and kinetic energies. The rate at which energy is transported in the direction of wave propagation across a vertical plane perpendicular to the direction of wave advancement and extending downward to the maximum depth is called energy flux (or, frequently, wave power). To estimate the flux of these energies, consider the right-hand vertical side of the slice of water in the column (a window with cross-section $\Delta z \Delta y$; (Fig. 2).

ISSN (Print): 2413-5267
ISSN (Online): 2706-9966

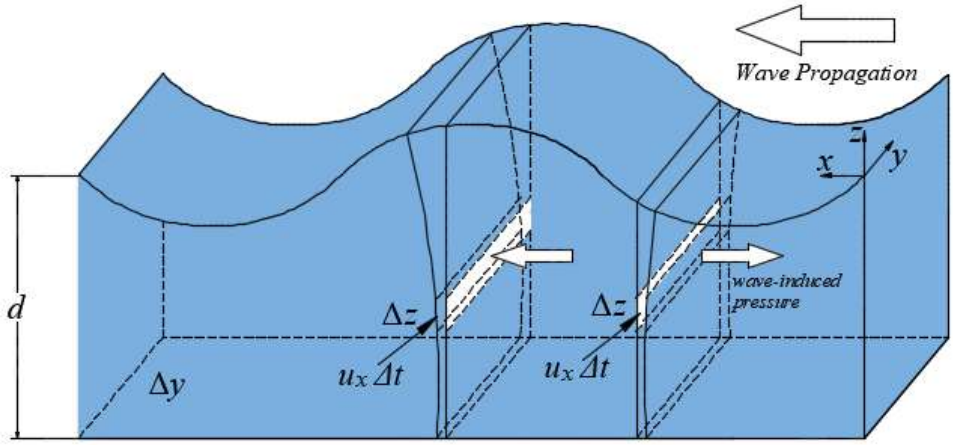

Figure 2. Horizontal flux of the wave energy.

The physical flux of potential energy ρgz through that slice in the x-direction (with the water particles, and therefore, with velocity u_x) in time interval (Δt) is given as $(\rho gz)u_x\Delta z\Delta y\Delta t$. Over the entire depth, from the bottom to surface, this energy flux (power) is calculated as;

$$P_{po} = \left(\int_{-d}^{\eta}(\rho gz)u_x\ dz\right)\Delta y\Delta t \quad \ldots\ldots (5)$$

where η is the displacement of water surface relative to still water level.

Similarly, the physical flux of the kinetic energy, that is, $0.5\rho u^2$, integrated over the entire depth, is calculated as;

$$P_k = \left(\int_{-d}^{\eta}\left(\frac{1}{2}\ \rho\ u^2\right)u_x\ dz\right)\Delta y\Delta t \quad \ldots\ldots (6)$$

In addition to the physical flux of the potential and kinetic energies, energy is also transported horizontally by the work done through the pressure in the direction of wave propagation. This horizontal flux through a vertical plane in time interval (Δt) is equal to the pressure (p_{wave}) multiplied by the distance moved in that interval (in the x-direction; $u_x\ \Delta t$). By integrating from the bottom to surface, the wave energy transported horizontally by the work done through pressure is written as;

$$P_{pr} = \left(\int_{-d}^{\eta}(pu_x)\ dz\right)\Delta y\Delta t \quad \ldots\ldots (7)$$

where $p = -\rho gz + p_{wave}$ and p_{wave} is the wave-induced pressure.

The total energy flux or total incident wave power ($P_{I.tot}$) per unit crest length and per unit time (i.e., divided by $\Delta y.\Delta t$) and time-averaged can be written as the sum of the three contributions as;

$$P_{I.tot} = \overline{P_{po}} + \overline{P_k} + \overline{P_{pr}} \quad \ldots\ldots (8)$$

ISSN (Print): 2413-5267
ISSN (Online): 2706-9966

The time-averaged energy fluxes given in Eqn. (8) were evaluated by Dean and Dalrymple (1991) and Holthuijsen (2010), and can be estimated as;

$$P_{I.tot} = \overline{\int_{-d}^{\eta}(\rho g z)u_x\ dz} + \overline{\int_{-d}^{\eta}\left(\frac{1}{2}\ \rho\ u^2\right)u_x\ dz} + \overline{\int_{-d}^{\eta}(-\rho g z + p_{wave})\,u_x\,dz} \quad \ldots\ldots (9)$$

The potential part of the wave power ($\rho g z.u_x$) given by the first term on the right-hand side of Eq. (9) cancels out the hydrostatic pressure ($-\rho g z.u_x$) given by the third term. The wave-induced pressure p_{wave} is in phase with the horizontal orbital motion and the surface elevation (Fig. 2). If the water particles move in the wave direction, the surface elevation is higher than when the water particles move against the wave direction. Therefore, the net time-averaged effect is an energy flux in the wave direction (Holthuijsen, 2010).

For most applications of linear wave theory, the second term is ignored as the integration is limited to a second-order approximation and the kinetic part of the wave energy flux is of third order. Nevertheless, this study considered this part of the wave power because it is expected to substantially increase the magnitude of the total transmitted wave power when added under the structure to the kinetic energy flux owing to the heaving behavior of the floating body. This expectation is based on the fact that the floating structures investigated in this research (*i.e.*, FBs and WECs) are usually installed in deep water and facing large amplitude waves. Under such conditions, the FBs are needed to attenuate the wave impact and the WECs are installed to capture more wave energy. The wave kinetic energy transport is associated with the wave amplitude which as it increases a higher magnitude of the wave energy transport obtained.

Therefore, the total incident wave power can be evaluated as;

$$P_{I.tot} = \overline{\int_{-d}^{\eta}\left(\frac{1}{2}\ \rho\ u^2\right)u_x\ dz} + \overline{\int_{-d}^{\eta}(p_{wave})\,u_x\,dz} \quad \ldots\ldots (10)$$

Based on the assumptions of linear wave theory, integration from the seabed to the still water level results in the final form of the total incident wave power:

$$P_{I.tot} = \overline{\int_{-d}^{0}\left(\frac{1}{2}\ \rho\ u^2\right)u_x\ dz} + \overline{\int_{-d}^{0}(p_{wave})\,u_x\,dz} \ = P_{I.1} + P_{I.2} \quad \ldots\ldots (11)$$

By deriving each part of Eqn. (11) separately, Alamailes and Turker (2019) found out that the last form of the kinetic part of the wave power is obtained as;

$$P_{I.1} = \frac{\rho g H^3\,\omega}{24}\left(\frac{\left(\sinh^2(kd)+3\right)}{\sinh(2kd)}\right) \quad \ldots\ldots (12)$$

Meanwhile, the second part of Eqn. (11), was evaluated in detail by Holthuijsen (2010) and the resulting wave power was obtained through Eqn. (3). Therefore, the total incident wave power is;

ISSN (Print): 2413-5267
ISSN (Online): 2706-9966

$$P_{I.tot} = P_{I.1} + P_{I.2} = \frac{\rho g H^3 \omega}{24}\left(\frac{(\sinh^2(kd)+3)}{\sinh(2kd)}\right) + \frac{\rho g H^2 \omega}{16k}\left[1 + \frac{2kd}{\sinh(2kd)}\right] \quad \ldots\ldots (13)$$

The first part of Eqn. (13) shows that $P_{I.1}$ is in third order of the wave amplitude. This makes this part negligible comparing to the second part ($P_{I.2}$) for waves with small amplitudes. However, this study suggests to take $P_{I.1}$ in consideration since in the typical wave conditions, under which the FBs usually installed, the wave amplitudes are relatively large and the water is deep. In these conditions, the linear wave theory is still applicable and $P_{I.1}$ magnitude fairly increases. For instance, in the North Sea the wave height reaches 5 m (Kramer and Frigaard, 2002) and if considering H = 4 m in deep water, $P_{I.1}$ will form about 10% of the total wave power. This amount should not be ignored when evaluating the transmitted wave power and hence K_t, and should be counted in when estimating the wave power for energy production.

4. Transmitted Power

The transmitted wave power is obtained by integrating the wave-induced pressure energy flux and the incident wave kinetic energy flux from the draft of the floating structure -*D* to the seabed -*d*. The kinetic energy flux from the floating structure's heaving oscillation is also added to the transmitted power.

4.1. Transmitted Wave Power

By referring to Eqn. (11) and integrating from the draft of the floating structure -*D* to the seabed -*d*, the kinetic energy contribution to the transmitted wave power ($P_{T.1}$) can be obtained as;

$$P_{T.1} = \overline{\int_{-d}^{-D}\left(\frac{1}{2}\rho u^2\right)u_x\, dz} = \frac{\rho g H^3 \omega}{48}\left[\frac{\tanh(kd)\sinh(k(d-D))(\sinh^2(k(d-D))+3)}{\sinh^3(kd)}\right] \quad \ldots\ldots (14)$$

Similarly, integrating the second part of Eqn. (11) from -*D* to -*d*, the transmitted induced pressure energy contribution to the transmitted wave power ($P_{T.2}$) is;

$$P_{T.2} = \overline{\int_{-d}^{-D}(p_{wave})\,u_x\, dz} = \frac{\rho g H^2 \omega}{16k}\left[\frac{(\sinh(2k(d-D))+2k(d-D)}{\sinh(2kd)}\right] \quad \ldots\ldots (15)$$

4.2. Floating Structure Mass and Hydrodynamic Mass Kinetic Energy Flux

Kinetic energy flux ($P_{T.3}$) (per unit width of the floating structure), produced by the heaving oscillation of the floating structure, increases the magnitude of the transmitted power. It consists of two parts: i) the kinetic energy flux from the heaving body of the floating structure, and ii) the kinetic energy flux from the hydrodynamic mass that accelerates simultaneously with the floating body.

The added mass is defined as the fluid mass that accelerates along with the floating structure. Therefore, this additional mass must be accounted for when the structure mass is considered.

For the heaving motion, Ruol *et al*. (2013) estimated the hydrodynamic mass M_h as the volume of water under the floating structure, where the volume boundary is described by a

ISSN (Print): 2413-5267
ISSN (Online): 2706-9966

semicircle with a radius equal to half the width (*B*) of the structure. This estimation was made assuming that the buoyancy force is the only vertical force considered when calculating the moorings' stiffness. The body mass (M_b) is equal to the mass of the displaced water, so the total estimated mass may be evaluated as the sum of (M_b and M_h), as shown in Fig. (3).

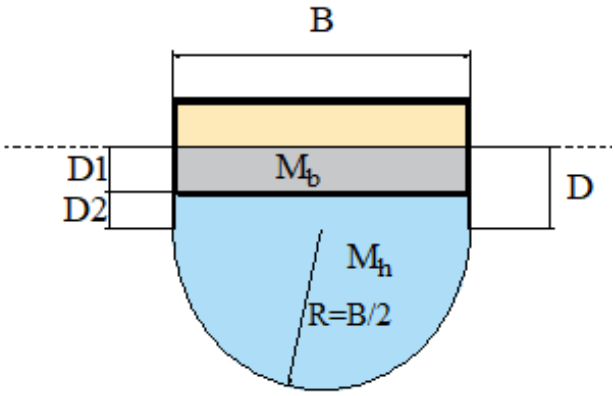

Figure 3. The estimated hydrodynamic mass for π-shaped floating structure (modified from Roul *et al*., 2013).

According to Fig. (3), the body mass (M_b) can be obtained using Archimedes' principle (per unit body length) (*i.e.*, $M_b = \rho\, B\, D_1$) and the hydrodynamic mass (M_h) can be obtained as;

$$M_h = \rho\, \frac{\pi}{8} B^2 + \rho\, B D_2 \qquad \ldots\ldots (16)$$

When estimating the kinetic energy flux (per unit structure width) resulting from the total accelerating mass, the shape of the added mass should be reconsidered to simplify the calculation. The added mass can be considered to be rectangular (as shown in Fig. 4) and can be fitted within the body width (*B*) and extended toward the seabed at depth (δ).

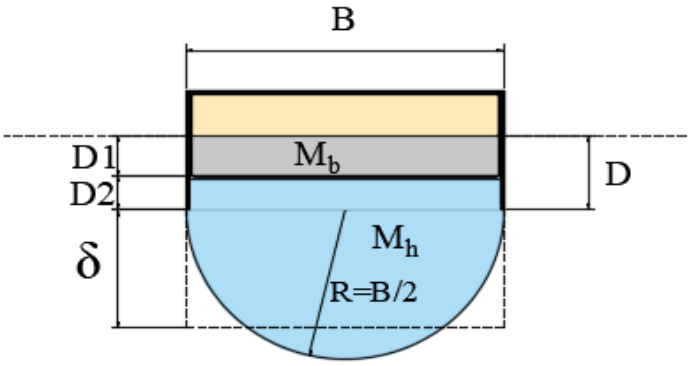

Figure 4. Simplified shape of the added mass for (a) π-shaped floating structure.

The cross-sectional area of the rectangular shape should be equal to the cross-sectional area of the semicircular shape. Such an arrangement provides equivalent added masses for both shapes. The equivalence of the masses can be achieved when the depth $\delta = (\pi/8) \times B$. Then, the hydrodynamic mass becomes;

ISSN (Print): 2413-5267
ISSN (Online): 2706-9966

$$M_h = \rho\, B(D_2 + \delta) \quad \ldots\ldots (17)$$

The kinetic energy flux generated by the structure's body (per unit body length) can be obtained by integrating ($0.5M_b \times u^2$) u_x from the still water level to the structure draft -D; the kinetic energy flux generated by the hydrodynamic mass can be obtained by integrating ($0.5M_h \times u^2$) u_x from -D to –($D_1 + D_2 + \delta$). The integrations are averaged over a wave period and per unit structure width as;

$$P_{T.3} = \int_{-D_1}^{0}(\tfrac{1}{2}\rho\, u^2)\, u_x\, dz + \int_{-D_2}^{-D_1}(\tfrac{1}{2}\rho\, u^2)\, u_x\, dz + \int_{-(D_1+D_2+\delta)}^{-D_2}(\tfrac{1}{2}\rho\, u^2)\, u_x\, dz \quad \ldots.. (18)$$

As the floating structure approaches the seabed, the hydrodynamic mass is apparently influenced by the close juxtaposition of the wall. Yamamoto *et al*. (1974) investigated the impact of the closeness of the seabed on the hydrodynamic mass of a cylinder, finding that, as the distance between the cylinder and seabed decreases, the hydrodynamic mass coefficient increases.

Therefore, Eqn. (18) is only valid for cases with shallow drafts and deep water, when the effect of the seabed on the hydrodynamic mass is negligible. However, for deeper drafts or shallower water, a correction factor (α) should be introduced to reflect the change in the added mass owing to the effect of closeness to the seabed. Therefore, $P_{T.3}$ can be considered (per unit structure width) to be;

$$P_{T.3} = \int_{-D_1}^{0}(\tfrac{1}{2}\rho\, u^2)\, u_x\, dz + \boldsymbol{\alpha}\left(\int_{-D_2}^{-D_1}(\tfrac{1}{2}\rho\, u^2)\, u_x\, dz + \int_{-(D_1+D_2+\delta)}^{-D_2}(\tfrac{1}{2}\rho\, u^2)\, u_x\, dz\right) \quad \ldots\ldots (19)$$

This study ignores the effect of the closeness of the seabed on the added mass (*i.e.*, $\alpha = 1$), as the formula is generalized for the deep-water conditions in which FBs are usually installed. For shallow depths or deep drafts, the value of α increases. When the floating body is large and is positioned at a depth less than or equal to its draft plus half of its width (i.e., $d \leq D + (B/2)$), the added mass can be assumed to be the mass trapped between the bottom of the structure -D and the seabed –d (see Fig. 3). However, under normal conditions (i.e., $d > D + (B/2)$), the added mass is extended to a depth of $\delta = (\pi/8)\, B$ (see Fig. 4).

Thus, Eqn. (19) is rewritten as;

$$P_{T.3} = \int_{-(D_1+D_2+\delta)}^{0}(\tfrac{1}{2}\rho\, u^2)\, u_x\, dz \quad \ldots\ldots (20)$$

The integration in Eqn. (20) is similar to that in the first term on the right and side of Eqn. (11), but with different integration limits. Therefore, by substituting the orbital velocities from linear wave theory and completing the integration steps, the following expression is obtained:

$$P_{T.3} = \frac{\rho\, gH^3\omega}{48}\left[\frac{\tanh(kd)\sinh\big(k(d+z)\big)\big(\sinh^2\big(k(d+z)\big)+3\big)}{\sinh^3(kd)}\right]_{-(D_1+D_2+\delta)}^{0} \quad \ldots\ldots (21)$$

Further, taking in consideration that ($D_1 + D_2 = D$) and plugging in the integration limits give;

$$P_{T.3} = \frac{\rho\, gH^3\omega}{48}\left[\left(\frac{\big(\sinh^2(kd)+3\big)}{\cosh(kd)\sinh(kd)}\right) - \frac{\tanh(kd)\sinh(k(d-(D+\delta)))\big(\sinh^2\big(k(d-(D+\delta))\big)+3\big)}{\sinh^3(kd)}\right] \quad (22)$$

ISSN (Print): 2413-5267
ISSN (Online): 2706-9966

When $D + [(\pi/8)\ B]$ is less than the water depth d, then $\delta = [(\pi/8)\ B]$. In this case, $P_{T.3}$ is given by;

$$P_{T.3} = \frac{\rho\, gH^3\omega}{48}\left[\left(\frac{\left(sinh^2(kd)+3\right)}{cosh(kd)\,sinh(kd)}\right) - \left(\frac{tanh(kd)sinh(k\left(d-D-\frac{\pi}{8}B\right)\left(sinh^2\left(k\left(d-D-\frac{\pi}{8}B\right)\right)+3\right)}{sinh^3(kd)}\right)\right] \quad \ldots\ldots (23)$$

In contrast, when $D + [(\pi/8)\ B]$ is greater than or equal to the water depth d, then $\delta = d\text{-}D$. In this case, $P_{T.3}$ is given by;

$$P_{T.3} = \frac{EH\omega}{3}\left(\frac{\left(sinh^2(kd)+3\right)}{sinh(2kd)}\right) \quad \ldots\ldots (24)$$

The total transmitted power obviously characterizes the wave power carried by a wave that passes the floating structure to the lee side. Naturally, the corresponding transmitted power ($P_{T.tot}$) is equivalent to the incident wave power propagating toward the shore, $P_{L.S}$, which can be calculated by Eqn. (18) as a function of transmitted wave height (H_t). The magnitude of $P_{L.S}$ is obtained as;

$$P_{T.1} \times L + P_{T.2} \times L + P_{T.3} \times B = P_{T.tot} \times L = P_{L.S} \times L \quad \ldots\ldots (25)$$

Hence, $P_{L.S}$ is a cubic function of the transmitted wave height (H_t). The cubic function always has three roots and, in this study, the leeside wave power ($P_{L.S}$) is always positive; therefore, there is always one real positive root for the equation, which is the resultant H_t. Once the value of H_t is obtained by solving Eqn. (13), K_t can be calculated using Eqn. (2).

5. Model Validation

The analytical model of this study was evaluated using laboratory data from two experimental researches on hydrodynamic performance of π-shaped FBs (Koutandos *et al*., 2005; and Cox *et al*., 2007). In addition, earlier theoretical approaches from Macagno (1954), Kriebel and Bollmann (1996), and Ruol *et al*. (2013) were evaluated using the same laboratory data; the results were compared with those of the approach proposed in this study.

Koutandos *et al*. (2005) experimental investigated the efficiency of box-type FB with attached impermeable plate which turned the FB to be π-shaped. The purpose of the study was to compare the hydrodynamic performance and the wave transmission behavior for the box and π-shaped structures. The tests were performed under the same settings that have been shown in Fig. (5).

ISSN (Print): 2413-5267
ISSN (Online): 2706-9966

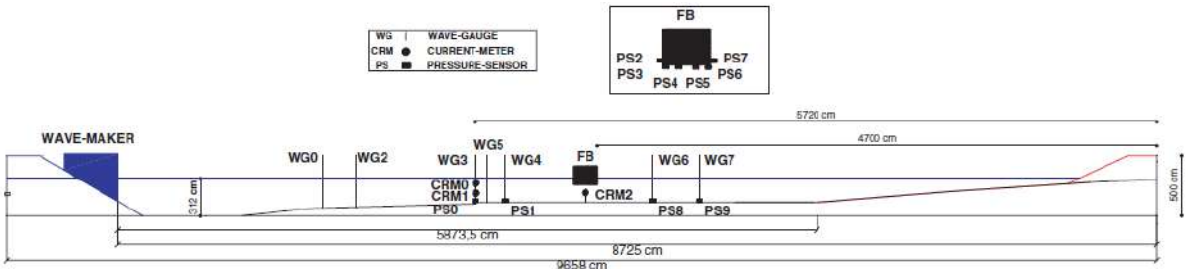

Figure 5. Dimensions of the CIEM Flume and the FB Position (Koutandos *et al*., 2005).

The total draft of the attached plate was meant to be the same as the draft of the box-type FB. Therefore, the keel of the box-type was reduced to give the FB the π-shape. The properties of the examined π-shaped FB and the wave conditions are shown in Table (1).

Table 1. π-shaped FB full-scale properties and regular wave conditions of Koutandos *et al*. (2005).

Model Scale	*Draft D (m)*		*Width B (m)*	*Incident Wave Height H_i (m)*	*Wave Period T (s)*	*Water depth d (m)*
	FB	**Plate**				
1:5	1	1	10	1.5	14.9, 12.4, 9.5, 7.5, 6.4, 5.4	10
	Total = 2					

Figure (6) shows a comparison between the experimental and theoretical transmission coefficients. The curves show the relationship between the relative floating structure width (B/L) and the transmission coefficient (K_t), as well as the relationship between the wave steepness H_i/L and K_t. In addition, the curves depict the relationship between K_t and the relative wave period T/T_n.

As shown in Figure (6), the calculated K_t using the present analytical model is in very good agreement with the experimental results of Koutandos *et al*. (2005) when $B/L < 0.19$, at which point an unexpected descent is observed in the measured data, possibly due to the natural period of the FB, which is ignored in theoretical approaches (Dong *et al*., 2008). Moreover, better correlation can be observed at a small wave steepness H_i/L which complies with the linear wave theory that is used in the derivations of the present approach. The relationship between K_t and the relative wave period T/T_n shows that the theoretical estimates deviate from the experimental measurement when the wave period becomes closer to the heave natural period. Generally, the theoretical results obtained from this study give the best estimation for K_t compared with the experimental results, whereas the models from Kriebel & Bollmann (1996), Macagno (1954), and Ruol *et al*. (2013) overestimate K_t.

ISSN (Print): 2413-5267
ISSN (Online): 2706-9966

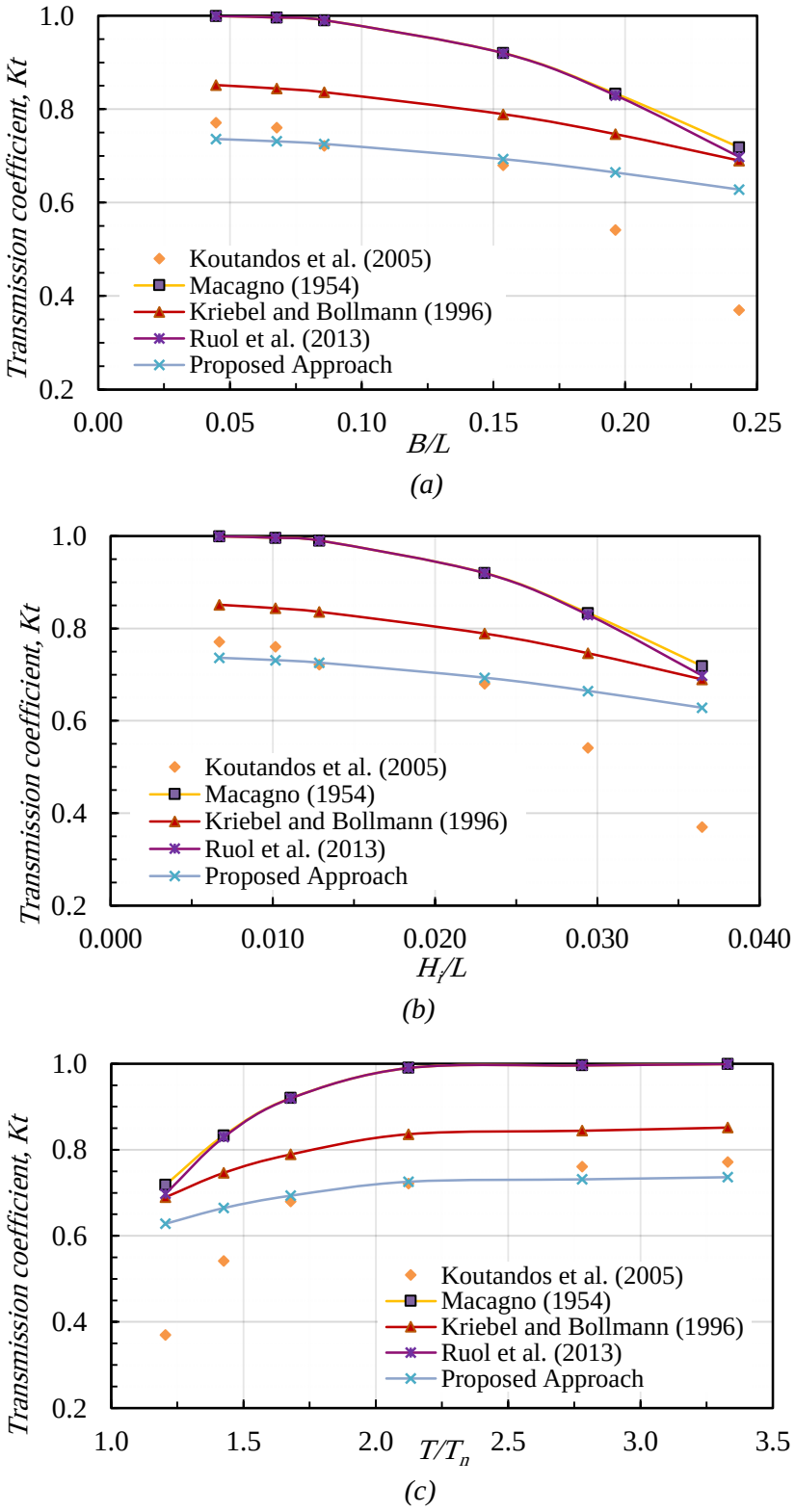

Figure 6. Change in the transmission coefficient of π-shaped FB with respect to; ***a)*** relative structure width *B/L;* ***b)*** Wave Steepness H_i/L*;* and ***c)*** relative wave period (T/T_n). The figure compares experimental results from Koutandos *et al*. (2005) with the outcomes of different theoretical approaches.

ISSN (Print): 2413-5267
ISSN (Online): 2706-9966

Cox *et al.* (2007) experimentally investigated the performance of pile restrained π-shaped FB under various wave conditions. The FB was restrained from horizontal movements while it was allowed to move in the vertical direction. The experimental investigation took a place in a wave flume at the University of New South Wales, Many Vale Water Research Laboratory. The flume was 130 m in length, 0.7 m in depth, and 0.6 m in width. The FB was positioned in the middle of the flume as shown in Fig. (7).

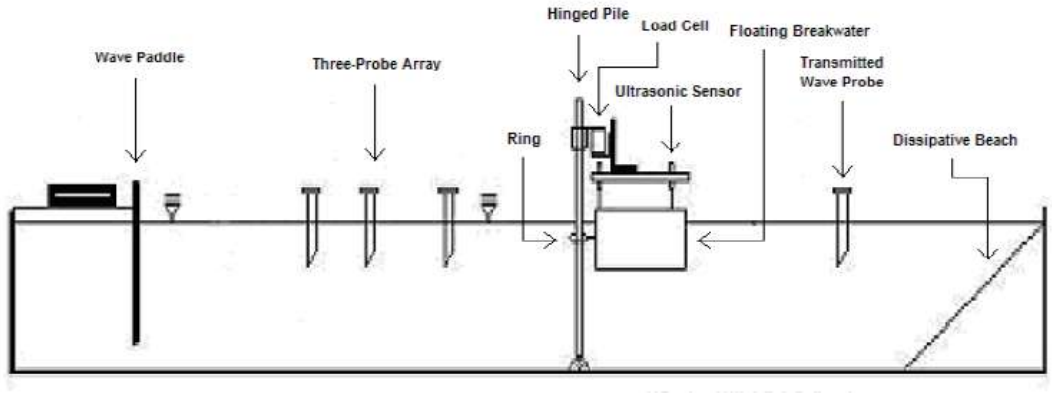

Figure 7. The set-up of the experiments for the FB (Cox *et al*., 2007).

The FB physical model is restrained by two piles which allow the structure to move vertically but limit its horizontal movement. The water depths and the details of the physical models employed in is summarized in Table (2).

Table 2. Full-scale properties of π-shaped FB and regular wave conditions of Cox *et al.* (2007).

Model Scale	*Draft D (m)*	*Width B (m)*	*Incident Wave Height H_i (m)*	*Wave Period T (s)*	*Water depth d (m)*
1:5	2.1	2.4	0.4, 0.8	2, 3, 4, 5	7

Figures (8) and (9) compare the experimental and theoretical transmission coefficients under two different incident wave heights (*i.e.*, H_i = 0.4 m and H_i = 0.8 m). The curves show the relationship between the relative floating structure width B/L and the transmission coefficient (K_t,) as well as the relationship between the wave steepness H_i/L and K_t. Furthermore, the curves present the relationship between K_t and the relative wave period T/T_n. As it can be observed in Fig. (8), the proposed model follows the trend of the measured results of Koutandos *et al*. (2005). The analytical approach gives the best K_t estimation when B/L is around 0.17 and slightly underestimates K_t when B/L is larger or smaller. Furthermore, excellent correlation can be observed at a wave steepness H_i/L= 0.03. The relationship between K_t and the relative wave period T/T_n shows that the analytical estimates are closer to the experimental measurements when the wave T/T_n is around 1.

ISSN (Print): 2413-5267
ISSN (Online): 2706-9966

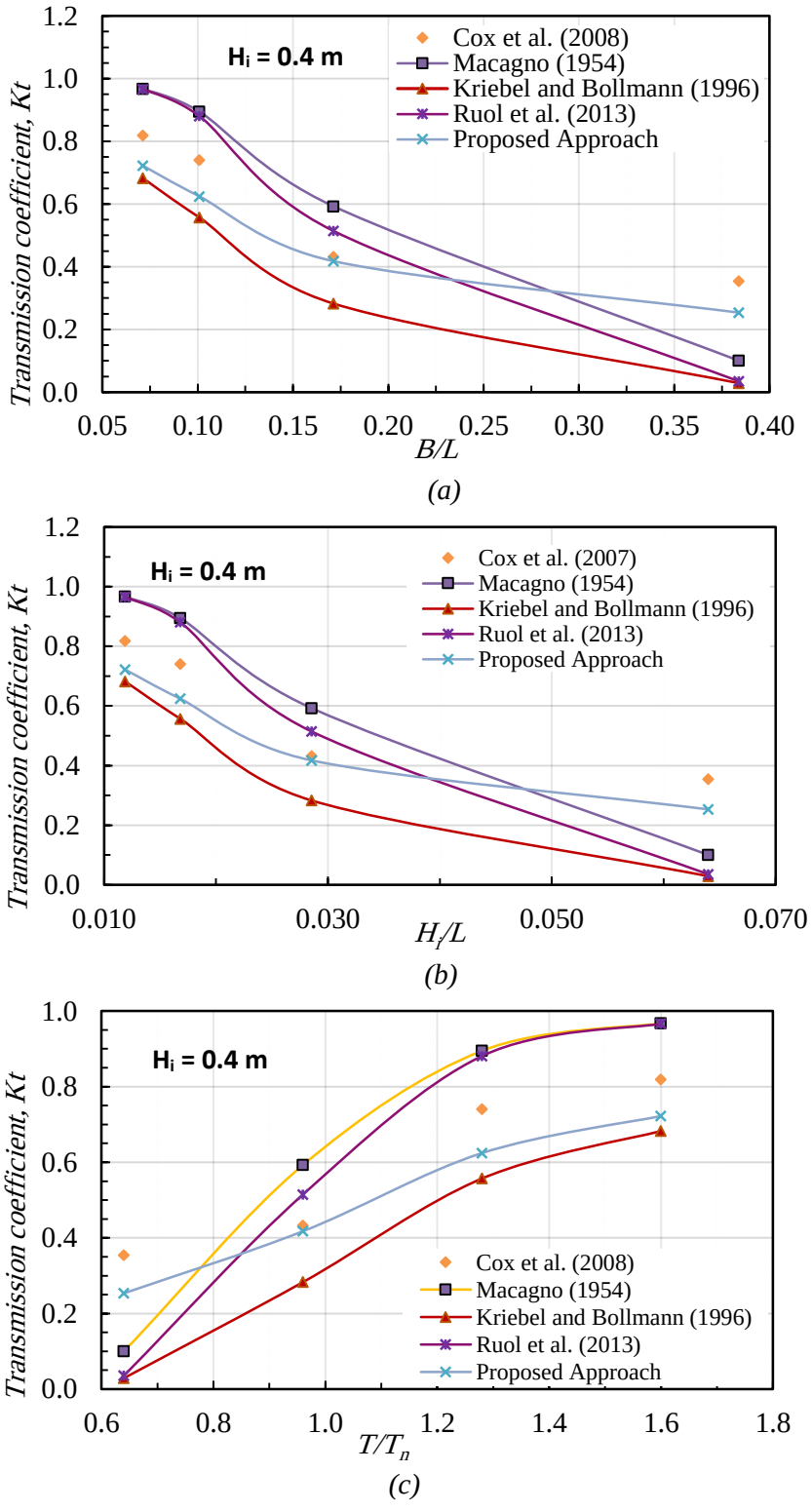

Figure 8. Change in the transmission coefficient of π-shaped FB with Respect to; **a)** Relative Structure Width *B/L*; ***b)*** Wave Steepness H_i/L; and **c)** relative wave period (T/T_n). The figure compares experimental results from Cox *et al*. (2007) with outcomes of different theoretical approaches when wave height H_i = 0.4 m.

ISSN (Print): 2413-5267
ISSN (Online): 2706-9966

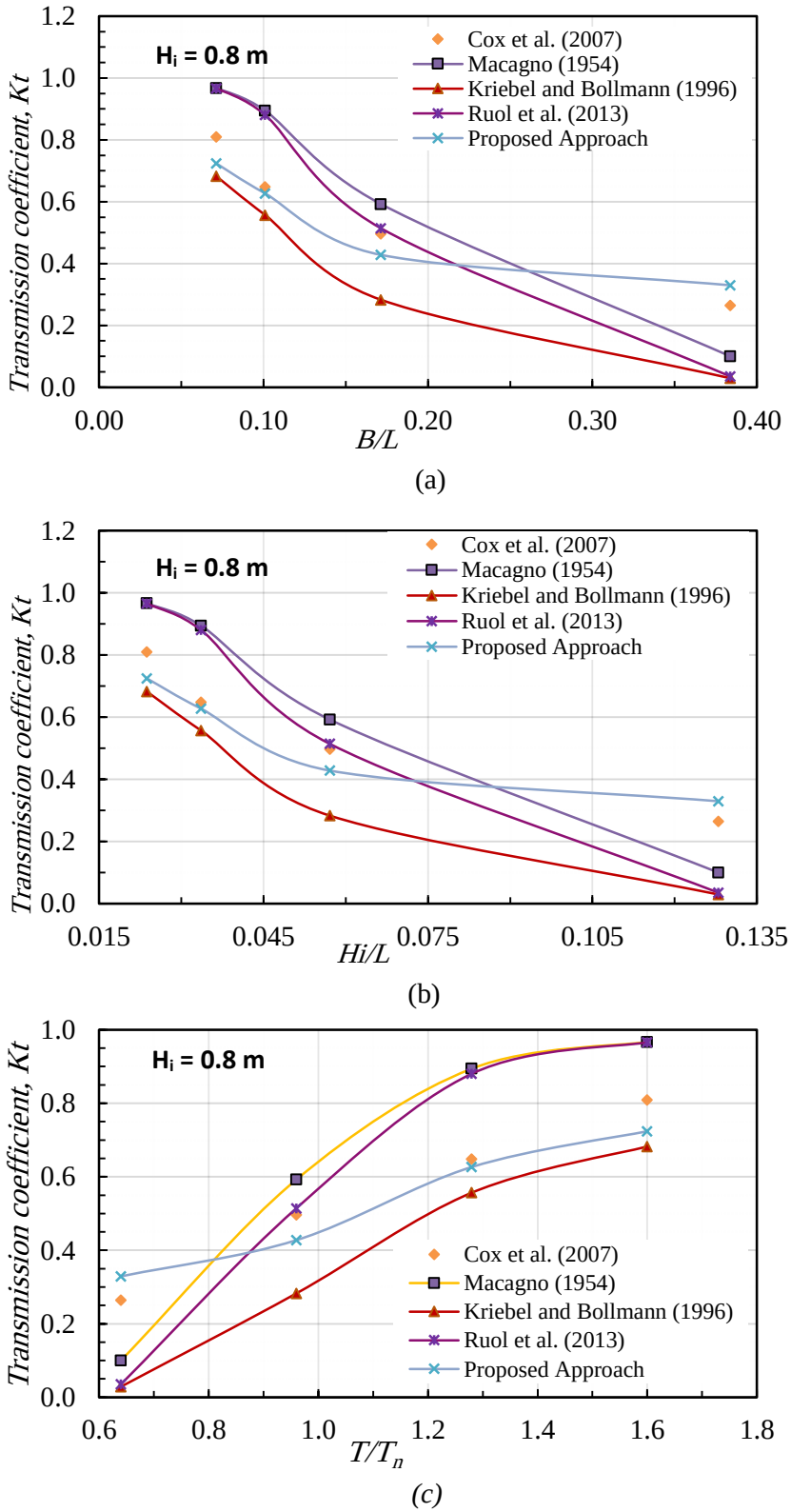

Figure 9. Change in the transmission coefficient of π-shaped FB with respect to; ***a)*** relative structure width B/L; ***b)*** wave steepness H_i/L; and ***c)*** relative wave period (T/T_n). The figure compares experimental results from Cox i. (2007) with outcomes of different theoretical approaches when wave height H_i = 0.8 m.

ISSN (Print): 2413-5267
ISSN (Online): 2706-9966

Similar outcomes can be seen in Figure (9). The analytical approach of this study gives a trend following curve to the measured data of Cox *et al*. (2007). However, a better correlation is obtained when the H_i = 0.8 m than when H_i = 0.4 m. Overall, the theoretical results obtained from this study gives the best estimations for K_t compared with the experimental results, whereas the models from Macagno (1954), Kriebel & Bollmann (1996), and Ruol *et al*. (2013) either overestimate or underestimate K_t.

An exceptional finding is obtained from the study of Cox *et al*. (2007) and it is shown in Table (3). The transmission coefficient calculated using all the theoretical models except the proposed approach remains constant even though the incident wave height is changed. The experimental results show a variation in the value of the transmission coefficient as the incident wave height increases from H_i = 0.4 to 0.8 m and the same results are obtained from the theoretical results of the analytical model of this study.

Table 3. The change in the measured and calculated transmission coefficient values for π-shaped floating structures with changing incident wave height.

Model	***Transmission Coefficient, K_t***							
	H_i = 0.4 m				***H_i = 0.8 m***			
	Wave Period (s)				***Wave Period (s)***			
	2	3	4	5	2	3	4	5
Cox *et al.* (2007)	0.35	0.43	0.74	0.82	0.26	0.50	0.65	0.81
Macagno (1954)	0.10	0.59	0.89	0.97	0.10	0.59	0.89	0.97
Kriebel and Bollmann (1996)	0.03	0.28	0.56	0.68	0.03	0.28	0.56	0.68
Ruol *et al.* (2013)	0.04	0.51	0.88	0.97	0.04	0.51	0.88	0.97
Proposed Approach	0.25	0.42	0.62	0.72	0.33	0.43	0.63	0.72

This finding is exclusively observed in the experimental study of Cox *et al*. (2007) since all the variables are kept constant except the incident wave height. The dimensions of the FB remained unchanged and the wave periods and wave depth were the same in all experimental tests.

6. Discussion

6.1. Comparison of Proposed and Available Models

Evaluations using the laboratory experimental data indicated that the proposed model estimates the transmission coefficient (K_t) well for smaller values of the relative structure width (i.e., *B/L*

ISSN (Print): 2413-5267
ISSN (Online): 2706-9966

≤ 0.2). However, as the relative structure width exceeds this limit, both the present approach and existing theoretical approximations overestimate K_t, which may result from scale effects on the behavior of the floating structure. Fig. (10) compares the measured and calculated transmission coefficients for the four aforementioned experimental studies and the four theoretical approaches (including the proposed model). In the case of Koutandos *et al*. (2005), it can be observed that the present model gives the closest expectations to measured K_t, especially under long wave conditions (*i.e*., $B/L < 0.2$); meanwhile, all the other theories produce overestimated values. In the case of the case of Cox *et al*. (2007), the present approach also gives the best K_t estimations and the lowest mean square error between the calculated and measured values which can be seen in Table (4).

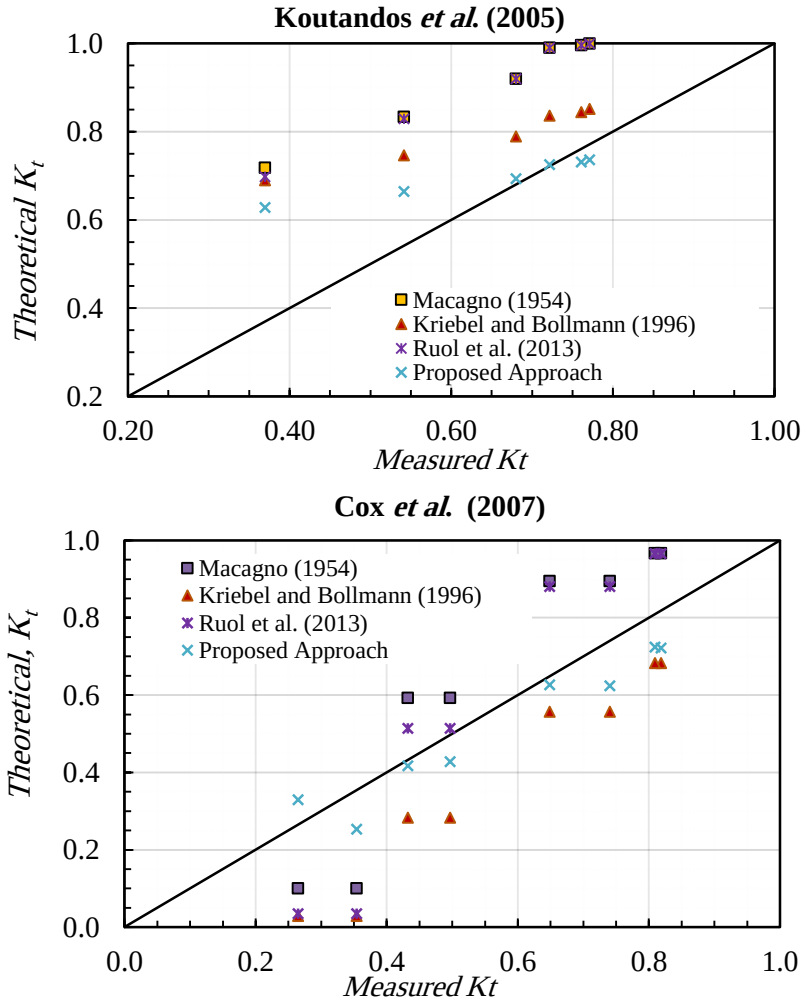

Figure 10. Measured versus calculated transmission coefficients for different applications using several theoretical models for π-shaped FB.

A better correlation between the present theory and the experimental results can be seen in case of the study of Cox *et al*. (2007) since the FB was allowed to oscillate vertically with more freedom than in the case of Koutandos *et al*. (2005).

ISSN (Print): 2413-5267
ISSN (Online): 2706-9966

Table 4. The mean square error between the measured and calculated transmission coefficient values for π-shaped floating structures.

Model	Koutandos *et al.* (2005)	Cox *et al.* (2007)
Macagno (1954)	0.074	0.032
Kriebel and Bollmann (1996)	0.031	0.038
Ruol et al. (2013)	0.071	0.035
Proposed Approach	0.014	0.006

6.2. Effect of Draft and Water Depth

The floating structure, which is used as wave attenuator, can be extended downward to the seabed to block nearly all the incident wave power, but as it is basically floating, the draft depth is typically much smaller than the water depth. In the case of short period waves, the orbital velocity decreases rapidly as the water depth increases. Hence, a deeper draft may not change the transmitted wave power. In contrast, the orbital velocity of long-period waves expands toward the seabed. Therefore, a larger draft is required to block the incident wave power. However, this situation is problematic owing to large possible mooring forces (Hals, 1981; and Oliver, 1994).

A deeper draft typically reflects more power and allows less energy to transfer to the lee side. The effect of relative draft on the transmission coefficient under constant wave climate and structure width has been determined using the proposed approach. The results show that as the draft increases (a higher value of *D/d*), the transmission coefficient decreases, indicating better blocking wave power transfer and successful additional attenuation of the transferred wave height (Fig. 11).

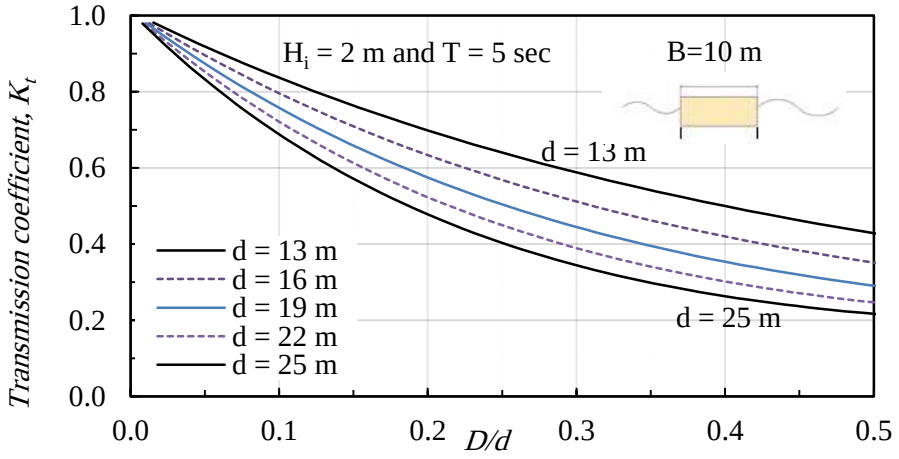

Figure 11. Effect of relative draft D/d on the transmission coefficient.

6.3. Effect of Incident Wave Height

In general, according to the definition of the transmission coefficient given in Eqn. (2), as the incident wave hits the floating structure, the transmitted percentage of the kinetic part of the

ISSN (Print): 2413-5267
ISSN (Online): 2706-9966

incident wave power and the induced pressure part of the incident wave power are constant. However, pursuant to the proposed methodology, the kinetic energy flux resulting from the oscillation of a heaving floating structure changes with the incident wave height. Fig. (12), which is plotted based on the proposed model of this study, shows that, under the same wave period condition, as the incident wave height increases, the transmission coefficient of the floating structure also increases. This result is expected, as the H_i is a factor that affects the calculation of the K_t. The kinetic energy flux resulting from the heaving movement of the floating structure and its hydrodynamic mass is a function of H_i, and it increases with wave height, leading to additional power transmission. Therefore, better wave attenuation (a lower value of K_t) is achieved in case of non-fixed floating structures experiencing short wave heights. This finding distinguishes the present model of this study from previous theoretical approaches, which ignored the effect of the incident wave height.

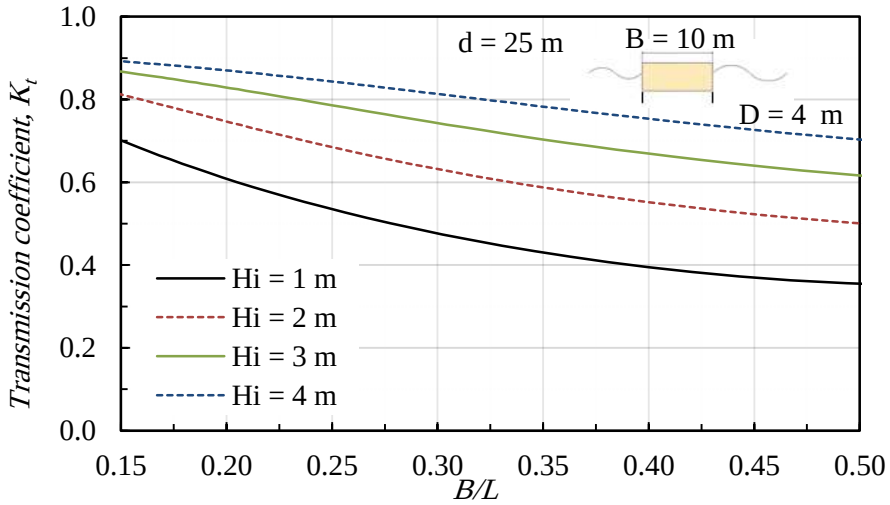

Figure 12. Effect of incident wave height Hi on the transmission coefficient

7. Conclusions

A numerical approach was developed to evaluate the wave attenuation capability of non-fixed floating structures. The proposed model was based on linear wave and power transmission theories, and it considers the effect of the structure's heaving oscillation. Because the model was developed based on a 2D assumption, diffraction effects due to the finite length of the floating structure were not considered. However, in practice, floating structures are usually connected to each other, or at least arranged such that they can be considered as a single long body. The proposed approach was validated using laboratory-scale experimental data obtained from the literature.

The results obtained using the proposed methodology of this research agreed with the small-scale results in the literature for waves with long periods and low steepness, in accordance with linear wave theory. Some scatter is to be expected, because it is difficult to adequately consider the effect of mooring stiffness in a simple approach. Part of the scatter is also attributed

ISSN (Print): 2413-5267
ISSN (Online): 2706-9966

to scale effects that are likely to influence the transmission behavior, especially for higher waves, ignoring overtopping. Therefore, this approach may be inaccurate when applied to waves higher than the freeboard of the floating structure.

Investigation on the effects of the floating structure draft and water depth indicated that at deeper drafts, the transmission coefficient of the floating structure decreases, and less power is transmitted to the lee side, thereby better reducing waves. In addition, for the same floating structure, wave attenuation achieved in deep water is better than that achieved in shallow water. Most significantly, this approach can be distinguished from other theoretical approaches proposed previously by the fact that H_i influences the calculation of the K_t via changes in the kinetic energy flux resulting from the heaving motions of the floating structure.

Notation

Symbol	Definition	Unit
B	floating structure width;	m
c	wave phase velocity;	m/s
D	floating structure draft;	m
d	water depth;	m
E	wave-induced energy per unit wave length;	J/m^2
E_k	wave kinetic energy per unit wave length;	J/m^2
E_{po}	wave potential energy per unit wave length;	J/m^2
g	gravitational acceleration;	m/s^2
H	wave height;	m
H_i	incident wave height;	m
H_s	significant wave height;	m
H_t	transmitted wave height;	m
k	wave number;	rad/m
K_t	transmission coefficient;	-
$K_{t.D.e}$	Wave Dragon experimental transmission coefficient;	-
L	wave length;	m
L_p	peak wave length;	m
M_b	floating body mass;	kg
M_h	hydrodynamic mass	kg
$P_{I.1}$	kinetic part of the incident wave power;	kW/m
$P_{I.2}$	induced pressure part of wave power;	kW/m
$P_{I.tot}$	total incident wave power;	kW/m
$P_{L.S}$	leeside wave power;	kW/m

ISSN (Print): 2413-5267
ISSN (Online): 2706-9966

$P_{T.1}$	kinetic energy contribution to the transmitted wave power;	kW/m
$P_{T.2}$	induced pressure energy contribution to the transmitted wave power;	kW/m
$P_{T.3}$	floating mass and added mass contribution to the transmitted wave power;	kW/m
$P_{T.tot}$	total transmitted power;	kW/m
p_{wave}	wave-induced pressure;	N/m^2
T	mean wave period;	s
T_n	natural period for heave oscillation;	s
T_p	peak wave period;	s
u_x	orbital velocity in the *x* direction;	m/s
u_z	orbital velocity in the *z* direction;	m/s
α	added mass correction factor;	-
δ	equivalent added mass depth;	m
η	displacement of water surface;	m
ρ	density of water;	kg/m^3
ω	wave circular or radian frequency.	1/s

References

Alamailes A. & Türker U. (2019). Using analytical approach to estimate wave transmission coefficient in floating structures. *Journal of Waterway, Port, Coastal, and Ocean Engineering*, *145*(3), 04019010.

Beels C. (2009). *Optimization of the lay-out of a farm of wave energy converters in the North Sea: Analysis of wave power resources, wake effects, production and cost*. Ph.D. thesis. Department of Civil Engineering, Ghent University.

Beels C., Troch P., De Visch K., Kofoed J.P., and De Backer G. (2010). Application of the time-dependent mild-slope equations for the simulation of wake effects in the lee of a farm of wave dragon wave energy converters. *Renewable Energy*, 35(8): 1644–1661.

Burcharth H.F., Zanuttigh B., Andersen T.L., Lara J.L., Steendam G.J., Ruol P., ... & Higuera P. (2015). Innovative engineering solutions and best practices to mitigate coastal risk. In: *Coastal risk management in a changing climate*. Butterworth-Heinemann., pp. 55-170.

Dean R.G. and Dalrymple R.A. (1991). *Water wave mechanics for engineers and scientists*, Vol. 2. World Scientific Publishing Company, Singapore.

Diaconu S. and Rusu E. (2013). The environmental impact of a wave dragon array operating in the Black Sea. *Sci. World J*., 498013.

Diamantoulaki I. and Angelides D.C. (2011). Modeling of cable-moored floating breakwaters connected with hinges. *Eng. Struct*., 33(5): 1536–1552.

ISSN (Print): 2413-5267
ISSN (Online): 2706-9966

Dong G., Zheng Y., Li Y., Teng B., Guan C., and Lin D. (2008). Experiments on wave transmission coefficients of floating breakwaters. *Ocean Eng.*, 35(8): 931–938.

Goggins J. and Finnegan W. (2014). Shape optimisation of floating wave energy converters for a specified wave energy spectrum. *Renewable Energy*, 71: 208–220.

Hales L.Z. (1981). *Floating breakwaters: State-of-the-art literature review*. Technical Rep. TR81-1. United States Army Corps of Engineers, Springfield, VA.

He F., Huang Z., and Law A.W. (2012). Hydrodynamic performance of a rectangular floating breakwater with and without pneumatic chambers: An experimental study. *Ocean Eng.*, 51: 16–27.

Holthuijsen L.H. (2010). *Waves in oceanic and coastal waters*. Cambridge University Press, Cambridge, U.K.

Ji C., Chen X., Cui J., Yuan Z., and Incecik A. (2015). Experimental study of a new type of floating breakwater. *Ocean Eng.*, 105: 295–303.

Kramer M.M. & Frigaard P.B. (2002). Efficient wave energy amplification with wave reflectors. *Proc. 12th Int. Offshore and Polar Eng. Conf.*, Kitakyushu, Japan, 707–712.

Kriebel D.L. & Bollmann C.A. (1996). Wave transmission past vertical wave barriers. *Proc. 25th Int. Conf. on Coastal Eng. (ICCE)*, ASCE, Reston, Va., 2470–2483.

Koutandos E., Prinos P., and Gironella X. (2005). Floating breakwaters under regular and irregular wave forcing: Reflection and transmission characteristics. *J. Hydraulic Res.*, 43(2): 174–188.

Li D., Panchang V., Tang Z., Demirbilek Z., and Ramsden J. (2005). Evaluation of an approximate method for incorporating floating docks in harbor wave prediction models. *Can. J. Civ. Eng.*, 32(6): 1082–1092.

Macagno E.O. (1954). Houle dans un canal présentant un passage en charge. *La Houille Blanche*, 1(1): 10–37 (in French).

Martinelli L., Ruol P., and Zanuttigh B. (2008). Wave basin experiments on floating breakwaters with different layouts. *Appl. Ocean Res.*, 30(3): 199–207.

McCartney B.L. (1985). Floating breakwater design. *J. Waterway Port Coastal Ocean Eng.*, 111(2): 304–318.

Ning D., Zhao X., Göteman M., and Kang H. (2016). Hydrodynamic performance of a pile-restrained WEC-type floating breakwater: An experimental study. *Renewable Energy*, 95: 531–541.

Nørgaard J.H. & Andersen T. L. (2012). Investigation of wave transmission from a floating wave dragon wave energy converter. *22nd Int. Offshore and Polar Eng. Conf.*, International Society of Offshore and Polar Engineers.

Oliver J., Aristaghes P., Cederwall K., Davidson D., De Graaf F., Thackery M., and Torum A. (1994). *Floating breakwaters: A practical guide for design and construction*. PIANC Report, Working Group 13, Permanent International Association of Navigation Congresses, Belgium.

ISSN (Print): 2413-5267
ISSN (Online): 2706-9966

Palha A., Mendes L., Fortes C.J., Brito-Melo A., and Sarmento A. (2010). The impact of wave energy farms in the shoreline wave climate: Portuguese pilot zone case study using pelamis energy wave devices. *Renewable Energy*, 35(1): 62–77.

Ruol P., Martinelli L., and Pezzutto P. (2013). Formula to predict transmission for π-type floating breakwaters. *J. Waterway Port Coastal Ocean Eng.*, 1–8.

Ruol P., Martinelli L., and Pezzutto P. (2013). Limits of the new transmission formula for pi-type floating breakwaters. *Coastal Eng. Proc.*, 1(33): 47.

Ruol P., Zanuttigh B., Martinelli L., Kofoed P., and Frigaard P. (2011). Near-shore floating wave energy converters: Applications for coastal protection. *Coastal Eng. Proc.*, 1(32): 61.

Sorensen R.M. (2005). *Basic coastal engineering*. Springer Science & Business Media, Berlin/Heidelberg, Germany.

Tsay T.K. & Liu P.L. (1983). A finite element model for wave refraction and diffraction. *Applied Ocean Research*, 5(1): 30-37.

Türker U. & Kabdasli M. (2004). Average sediment dislocation analysis for barred profiles. *Ocean Eng.*, 31(14): 1741–1756.

Türker U. (2014). Excess energy approach for wave energy dissipation at submerged structures. *Ocean Eng.*, 88: 194–203.

Ursell F. (1947). The effect of a fixed vertical barrier on surface waves in deep water. *Math. Proc. Cambridge*, 43(3): 374–382.

Venugopal V. & Smith G.M. (2207). Wave climate investigation for an array of wave power devices. *Proceedings of the 7th European wave and tidal energy conference*, Porto, Portugal, 11-14.

Wiegel R.L. (1960). Transmission of waves past a rigid vertical thin barrier. *J. Waterways Harbors Div.*, 86(1): 1–12.